Annals of Botany **114**: 1279–1294, 2014
doi:10.1093/aob/mcu053, available online at www.aob.oxfordjournals.org

ANNALS OF BOTANY
Founded 1887

PART OF A SPECIAL ISSUE ON PLANT CELL WALLS

Pectic-β(1,4)-galactan, extensin and arabinogalactan–protein epitopes differentiate ripening stages in wine and table grape cell walls

John P. Moore[1,*], Jonatan U. Fangel[2], William G. T. Willats[2] and Melané A. Vivier[1]

[1]*Institute for Wine Biotechnology, Department of Viticulture and Oenology, Faculty of AgriSciences, Stellenbosch University, Matieland 7602, South Africa and* [2]*Department of Plant and Environmental Sciences, Faculty of Science, University of Copenhagen, Copenhagen DK-1001, Denmark*

** For correspondence. E-mail moorejp@sun.ac.za*

Received: 14 November 2013 Returned for revision: 17 January 2014 Accepted: 26 February 2014 Published electronically: 7 May 2014

• **Background and Aims** Cell wall changes in ripening grapes (*Vitis vinifera*) have been shown to involve re-modelling of pectin, xyloglucan and cellulose networks. Newer experimental techniques, such as molecular probes specific for cell wall epitopes, have yet to be extensively used in grape studies. Limited general information is available on the cell wall properties that contribute to texture differences between wine and table grapes. This study evaluates whether profiling tools can detect cell wall changes in ripening grapes from commercial vineyards.

• **Methods** Standard sugar analysis and infra-red spectroscopy were used to examine the ripening stages (green, véraison and ripe) in grapes collected from Cabernet Sauvignon and Crimson Seedless vineyards. Comprehensive microarray polymer profiling (CoMPP) analysis was performed on cyclohexanediaminetetraacetic acid (CDTA) and NaOH extracts of alcohol-insoluble residue sourced from each stage using sets of cell wall probes (mAbs and CBMs), and the datasets were analysed using multivariate software.

• **Key Results** The datasets obtained confirmed previous studies on cell wall changes known to occur during grape ripening. Probes for homogalacturonan (e.g. LM19) were enriched in the CDTA fractions of Crimson Seedless relative to Cabernet Sauvignon grapes. Probes for pectic-β-(1,4)-galactan (mAb LM5), extensin (mAb LM1) and arabinogalactan proteins (AGPs, mAb LM2) were strongly correlated with ripening. From green stage to véraison, a progressive reduction in pectic-β-(1,4)-galactan epitopes, present in both pectin-rich (CDTA) and hemicellulose-rich (NaOH) polymers, was observed. Ripening changes in AGP and extensin epitope abundance also were found during and after véraison.

• **Conclusions** Combinations of cell wall probes are able to define distinct ripening phases in grapes. Pectic-β-(1,4)-galactan epitopes decreased in abundance from green stage to véraison berries. From véraison there was an increase in abundance of significant extensin and AGP epitopes, which correlates with cell expansion events. This study provides new ripening biomarkers and changes that can be placed in the context of grape berry development.

Key words: Profiling, berry ripening, plant cell wall, pectic-β-(1,4)-galactan, extensin, arabinogalactan–protein, AGP, wine grapes, table grapes, *Vitis vinifera*, Cabernet Sauvignon, Crimson Seedless.

INTRODUCTION

Understanding the processes controlling and influencing the ripening behaviour of fleshy fruits has been the goal of numerous investigations over many decades (Seymour *et al*., 2013*a*). It has become increasingly apparent that fruit ripening is much more complicated than a general uncontrolled degradation (i.e. melting) of the surrounding flesh as ripening proceeds to produce soft fruit (Seymour *et al*., 2013*a*). Much of our knowledge of fruit ripening has been gained from extensive study of *Solanum lycopersicum*, the cultivated tomato, which has resulted in a draft genome sequence (Zouine *et al*., 2012) and has supported the application of various omics technologies (Seymour *et al*., 2013*b*). Cell wall studies on tomato are also far advanced and so *S. lycopersicum* is generally considered the model fruit crop of choice in this regard (Seymour *et al*., 2013*b*). However, tomato is a climacteric fruit crop, and ripening continues even after detachment from the mother plant; this is not the case with all fruits (Ruiz-May and Rose, 2013; Seymour *et al*., 2013*a*). An important non-climacteric fruit is *Vitis vinifera*, the domesticated grapevine, which does not ripen off the vine (Creasy and Creasy, 2009; Davies *et al*., 2012). Grape development proceeds through a number of phenological stages; a few main way-points after flowering are fruit-set, with small green (pea-size) to larger green (berry touch) berries; véraison, when re-programming towards ripening starts (and when red grapes colour); and full ripe, when bunches are harvested (Creasy and Creasy, 2009). During ripening, grapes undergo distinct transcriptional (Davies and Robinson, 2000; Terrier *et al*., 2005, Fasoli *et al*., 2012), proteomic (Cramer *et al*., 2013; Martínez-Esteso *et al*., 2013) and metabolic (Ali *et al*., 2011; Dai *et al*., 2013) changes, the most common metabolite markers being the accumulation of sugars and organic acids (Coombe, 1960; Eyéghé-Bickong *et al*., 2012), anthocyanins and phenolics (Singleton and Trousdale, 1992; Cohen *et al*., 2012) and turnover of chlorophyll/carotenoids with the concomitant production of aroma volatiles (Martin *et al*., 2012; Young *et al*., 2012; Lashbrooke *et al*., 2013). It is becoming increasingly evident that the grape berry shows transcriptome 'plasticity' and that the expression of some genes is governed

by environmental–geographic considerations in addition to developmental patterning (Santo *et al*., 2013). Control of ripening is driven by transcriptional regulation (i.e. transcriptome changes), and hormones such as ABA, ethylene and gibberellins are major factors influencing maturation (Chervin *et al*., 2008; Davies *et al*., 2012; Fasoli *et al*., 2012; Young *et al*., 2012). A major challenge is the integration of different transcriptional, proteomic and metabolite datasets to more accurately model grape berry ripening dynamics (Fortes *et al*., 2011; Martínez-Esteso *et al*., 2013) and to relate this to the ongoing grapevine genome annotation activities (Jaillon *et al*., 2007; Grimplet *et al*., 2009).

Along with these changes, many grape varieties undergo turgor-related softening (Thomas *et al*., 2008). This is commonly observed with wine grapes; however, table grape varieties are known to remain firm and crisp (Creasy and Creasy, 2009). An obvious factor to consider is the contribution of cell wall changes during ripening (Ruiz-May and Rose, 2013); although grapes have been studied from this perspective in the past (Nunan *et al*., 1997, 1998; Vidal *et al*., 2001; Yakushiji *et al*., 2001; Doco *et al*., 2003*a*, *b*) many of these approaches are dated and knowledge gaps exist. Recent developments in the cell wall field have led to novel high-throughput methods to characterize large numbers of samples to support omics studies linked to biofuels research, plant–pathogen interactions and evolution studies (Albersheim *et al*., 2011; Persson *et al*., 2011). In this study we applied cell wall profiling tools (Moller *et al*., 2007; Moore *et al*., 2014) to characterize the compositional changes that occurred in a wine grape (Cabernet Sauvignon) versus a table grape (Crimson Seedless) cultivar as ripening proceeded. The study highlighted that certain cell wall probes (Hervé *et al*., 2011) show promise as ripening markers in grapes and appear to define key stages in both cultivars. Pectic-β-(1,4)-galactan epitopes associated with both cyclohexanediaminetetraacetic acid (CDTA) and NaOH fractions decreased in abundance in pre-véraison grapes. In contrast, extensin and arabinogalactan protein (AGP) epitopes increased at véraison. These changes appear to correlate with a transcriptional shift in berry metabolism linked to the onset of cell expansion. This pattern of epitope abundance also occurred in table grapes, except that higher relative abundance of homogalacturonan epitopes was noted. Berry ripening appears to fit into a conserved developmental framework in which genetic regulation probably plays a major role in cell wall events.

MATERIALS AND METHODS

Plant material and sampling

Samples of wine grapes were obtained from a *Vitis vinifera* Cabernet Sauvignon vineyard; the source clone CS 388C was grafted onto 101-14 Mgt (*Vitis riparia* × *V. rupestris*). The vineyard is situated (33°56′42″S, 18°51′44″E), close to the Eerste River on the Welgevallen experimental farm of Stellenbosch University. The vineyard is composed of alluvial soils with light to medium texture and is arranged in north–south row orientation. Vines are trained on a seven-wire vertical trellis system and are drip-irrigated. Samples of table grapes were obtained from a 5-year-old commercial vineyard (*V. vinifera* Crimson Seedless) located in the Paarl region (33°08′138″S, 18°59′138″E); the source clone C102-26 was grafted onto 'Richter 110' (*V. berlandieri* × *V. rupestris* 'Martin') rootstocks. Vine spacing was in an east–west orientation and trellised on a gable system with split cordons. Phenological stages and berry ripening were monitored experimentally (data not shown) by sampling and weighing berries for total soluble solids, expressed as degrees Brix (°Bx), using a refractometer, as well as pH and titratable acidity using a Metrohm 785 automated titrator (Metrohm AG, Switzerland) in order to determine the respective maturity index (data not shown). The Crimson Seedless vineyard received commercial hormone treatments [gibberellins and ethephon; Chervin *et al.* (2008)] during the season. Grapes are dipped in a gibberellic acid-rich solution to promote berry elongation and size, whereas ethylene (ethephon) is sprayed to promote colour development in red varieties. Sampling consisted of obtaining eight biological samples corresponding to eight individual vines over two vine rows at each stage; from two bunches per vine 16 berries were pooled to produce one sample; technical repeats were included in each analysis. Sampling occurred at green stage (berry touch, code L), then again at véraison (code M) and finally ripe (maturity, code N) just prior to harvest, according to the system proposed by Baillod and Baggiolini (1993).

Preparation of cell wall material from grape berries

Berries collected from the three developmental stages (green, véraison and ripe) were flash-frozen in liquid nitrogen in the field and stored at −80 °C prior to analysis. Pre-cooled (at liquid nitrogen temperature) samples were de-seeded manually (mainly

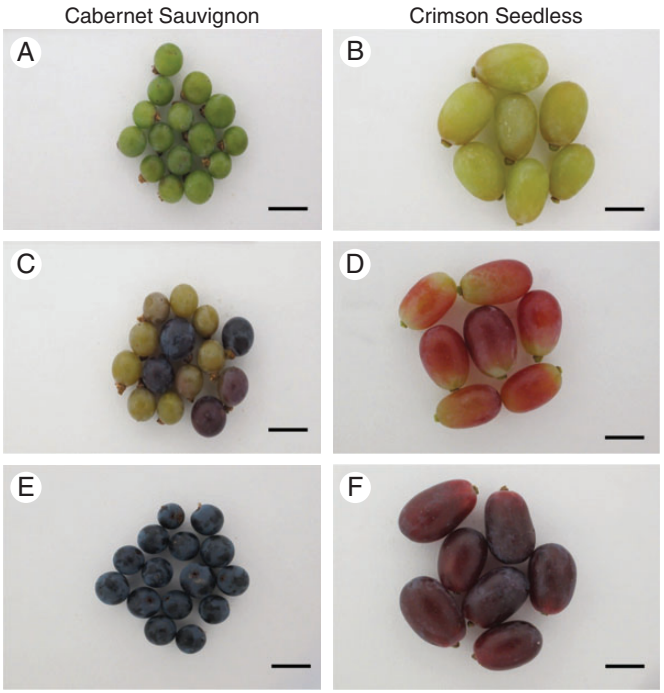

FIG. 1. Representative images of grape berries sourced from Cabernet Sauvignon (A, C, E) and Crimson Seedless (B, D, F) vineyards. Ripening stages green (berry touch) (A, B), véraison (C, D) and ripe (E, F), are shown. Scale bars = 1·5 cm. Stages correspond to K, M and N according to Baillod and Baggiolini (1993).

wine grapes; Cabernet Sauvignon) and skins and pulp were ground together to a fine powder using a mortar and pestle. Powdered samples (under liquid nitrogen) were transferred directly to boiling 80 % aqueous (v/v) absolute ethanol and boiled for 25 min to deactivate endogenous enzyme activity. Samples were transferred through a series of solvent washes in methanol, chloroform and acetone as outlined in Moore *et al.* (2014). After lyophilization, powdered samples (i.e. alcohol-insoluble residue, AIR) were stored at room temperature until further analysis.

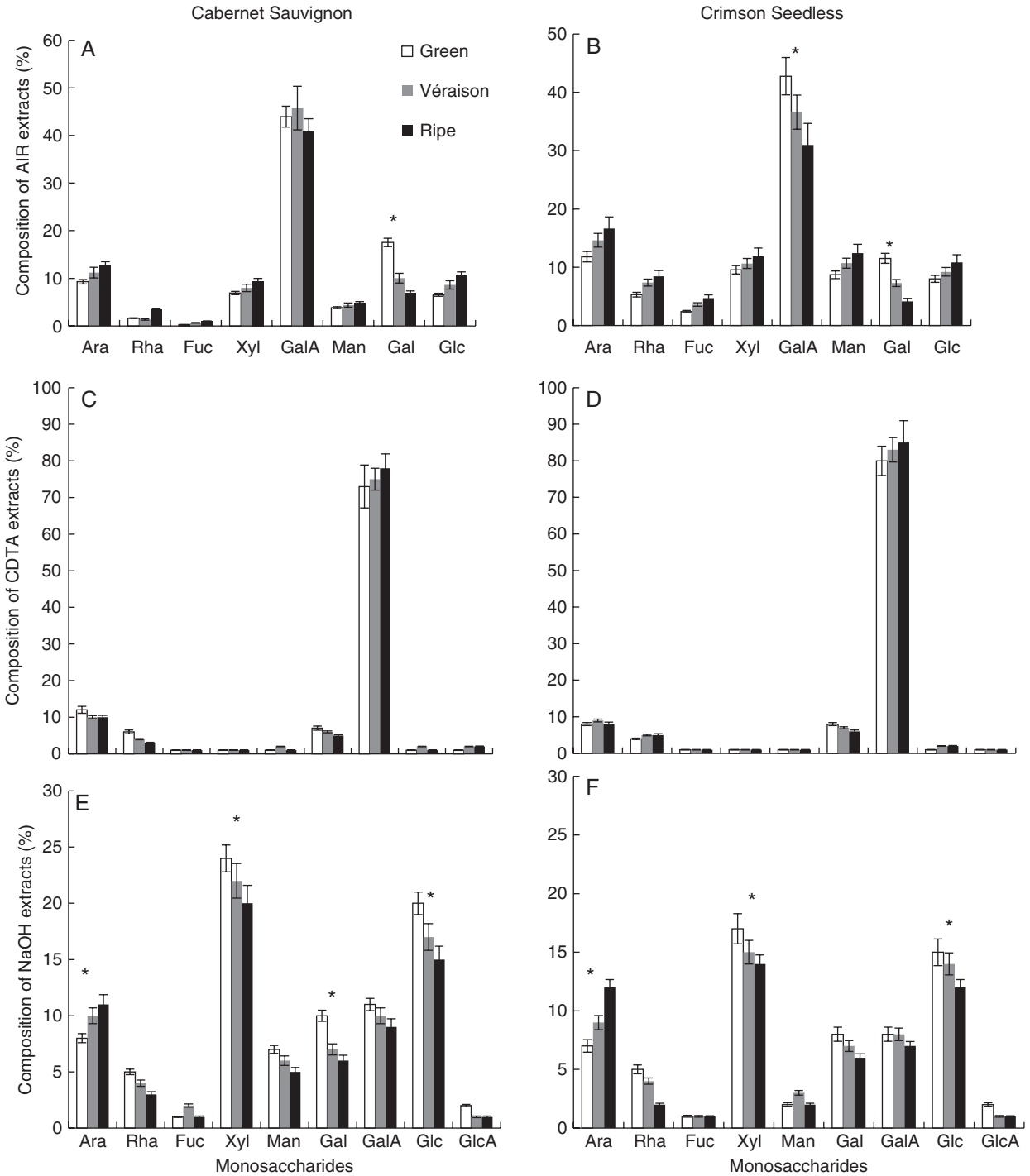

FIG. 2. Monosaccharide composition analysis of total AIR (A, B), CDTA extracts (C, D) and NaOH extracts (E, F) prepared from Cabernet Sauvignon (A, C, E) and Crimson Seedless (B, D, F) grape berries at different ripening stages. Ara, arabinose; Rha, rhamnose; Fuc, fucose; Xyl, xylose; Man, mannose; Gal, galactose; Glc, glucose, GalA, galacturonic acid; GlcA, glucuronic acid. Error bars represent the standard deviation of the mean for eight biological samples with two technical repeats per analysis. *Significant difference ($P < 0{\cdot}05$) between sample sets.

Sugar composition analysis using gas chromatography

To determine the composition and quantity of monosaccharides present in the non-cellulosic portion of AIR, a standard sugar analysis procedure was followed (Moore *et al*., 2014). Samples were hydrolysed in 2 M trifluoroacetic acid at 110 °C for 2 h before centrifugation and the supernatants were dried under vacuum. Hydrolysed material was derivatized first using methanolic HCl to produce methoxy sugars followed by silylation to produce trimethylsilyl glycosides (for the complete protocol see Nguema-Ona *et al*., 2012; Moore *et al*., 2014). A gas chromatography method first described by York *et al.* (1985), performed on a Hewlett Packard 5890 series II instrument, was used to separate and quantify the sugar derivatives obtained from the samples.

Vibrational reflectance spectroscopy of cell wall samples

A complete wavelength absorbance spectrum in the infra-red region from each sample was obtained directly from AIR. Powdered samples were placed directly (in contact mode) onto the diamond window and clamped in position to obtain reflectance spectra. A NEXUS 670 (Thermo, USA) instrument equipped with a Golden Gate Diamond ATR (attenuated total reflectance) accessory was used to record spectra (128 co-added scans per analysis) between 4000 and 650 cm^{-1} using a Geon-KBr beamsplitter and DTGS/Csl detector.

Comprehensive microarray polymer profiling analysis of cell wall fractions

Comprehensive microarray polymer profiling (CoMPP) was performed on AIR samples using a procedure outlined and described in Moller *et al.* (2007). Each analysis used approximately 10 mg of AIR, which was extracted sequentially with CDTA and then NaOH solutions to obtained pectin-rich and hemicellulose-rich extracts. Samples were sequentially extracted following 30 µl for each 1 mg of AIR for 2 h for both CDTA and NaOH. This involved a tissue-lyser, first at 27 shakes s^{-1} for 2 min and then down to 6 shakes s^{-1} for 120 min. A 50 mM CDTA solution was followed by 4 M NaOH with 0·1 % $NaBH_4$ to obtain an insoluble residue. These extracts were spotted onto membranes and then probed with monoclonal antibodies (mAbs) and carbohydrate-binding modules (CBMs) (Knox, 1997; Hervé *et al*., 2011) that recognize specific cell wall epitopes (detailed in Moller *et al*., 2007). Data were reported as a heat map, in which mean spot signals were displayed and the range was normalized to the highest signal (set as 100) in the dataset.

Multivariate and univariate statistics

Univariate descriptive statistics and one-way ANOVA were performed (with $P = 0{\cdot}05$) under the guidance of the Centre for Statistical Consultation (CSC) at Stellenbosch University (Professor Martin Kidd). Software packages used include Statistica 10 (Statsoft) and Excel 2010 (Microsoft). Multivariate methods, including principal component analysis (PCA), were performed using SIMCA (MSK Inc., U-metrics) software. Spectral [Fourier transform infra-red spectroscopy (FTIR)] and CoMPP datasets were imported into SIMCA (MSK Inc., U-metrics) using conversion algorithms. Spectral data were averaged after baseline correction, smoothing (Savitsky–Golay) and multiplicative scatter correction.

RESULTS

Ripening in grapes is a sequential process marked by defined stages according to traditional viticultural perspectives and practices (Baillod and Baggiolini, 1993; Creasy and Creasy, 2009). Initially berries develop from green (berry touch) stage (code L), when they are acidic and have a firm texture (Baillod and Baggiolini, 1993). Green berries undergo photosynthesis, are actively metabolizing (especially biosynthesis) and show high cell division rates. Once berries reach their developmentally programmed cell number they pass through a stage termed 'véraison' (code M); in red grapes this is accompanied by berry colouring caused by anthocyanin biosynthesis (Baillod and Baggiolini, 1993; Creasy and Creasy, 2009). Véraison is often asynchronous, individual berries in a bunch often being at different degrees of colour change; thus, a statistical bell-shaped population distribution is probably a good analogy, and so in viticulture the term has been difficult to define accurately (Lund *et al*., 2008). After véraison the berries enlarge, accumulate sugar (glucose and fructose) and soften (more so in wine grapes), producing ripe, sweet berries (stage code N) at harvest (Baillod and Baggiolini, 1993; Creasy and Creasy, 2009). Inspection of representative images of green (berry touch, code L), véraison (véraison, code M) and ripe (maturity, code N) berries of Cabernet Sauvignon (Fig. 1A, C, E) and Crimson Seedless (Fig 1B, D, F) berries revealed the typical ripening sequence. However, wine grapes are small and spherical, whereas table grapes are larger and elongated in shape. Moreover, table grapes are harvested physiologically earlier and are much firmer (with a crunchy texture) compared with wine grapes, which become substantially softer after véraison. Defining texture and grape quality is a complex field (Rolle *et al*., 2012) and it has been shown that numerous factors, including hormones (Peppi *et al*., 2006) and harvesting timing/treatments (Zouid *et al*., 2013), contribute to berry firmness. In the context of this study, cell wall composition is only one factor that contributes to texture and so any conclusions drawn need to be cautious and circumspect.

TABLE 1. *Gravimetric analysis of CDTA and NaOH extracts of alcohol-insoluble residue (AIR) from wine (Cabernet Sauvignon) and table (Crimson Seedless) grape berries*

	Cabernet Sauvignon	Crimson Seedless
CDTA		
Green	$21{\cdot}5 \pm 1{\cdot}8^{a}$	$34{\cdot}4 \pm 8{\cdot}0^{d}$
Véraison	$30{\cdot}8 \pm 6{\cdot}3^{b}$	$33{\cdot}9 \pm 5{\cdot}1^{d}$
Ripe	$30{\cdot}1 \pm 5{\cdot}2^{b}$	$24{\cdot}0 \pm 6{\cdot}6^{e}$
NaOH		
Green	$38{\cdot}7 \pm 4{\cdot}2^{c}$	$21{\cdot}8 \pm 5{\cdot}4^{e}$
Véraison	$41{\cdot}5 \pm 3{\cdot}6^{c}$	$20{\cdot}1 \pm 3{\cdot}1^{e}$
Ripe	$45{\cdot}9 \pm 7{\cdot}0^{cd}$	$28{\cdot}7 \pm 4{\cdot}1^{f}$

Data (mg per 100 mg AIR) represent mean and s.d. of the mean for $n = 8$ samples per cultivar per stage.

Different letters represent significant differences ($P < 0{\cdot}05$) between extract yields within each extraction set.

To determine if bulk cell wall yields and composition differ between the two cultivars, and thus may play a role in the observed texture differences, total (non-cellulosic) monosaccharide composition at each developmental stage was measured from total AIR, as well as CDTA and NaOH fractions (as performed in the CoMPP procedure). Total AIR was found to range between 5 and 10 % of total fresh hydrated berry weight in all stages. Monosaccharide composition of total AIR showed that berry cell walls from both cultivars and all developmental stages were marked by a large proportion of galacturonic acid (between ~40 and 50 mol %) (Fig. 2A, B), confirming the pectin-rich nature of the samples. Furthermore, the other monosaccharides assayed

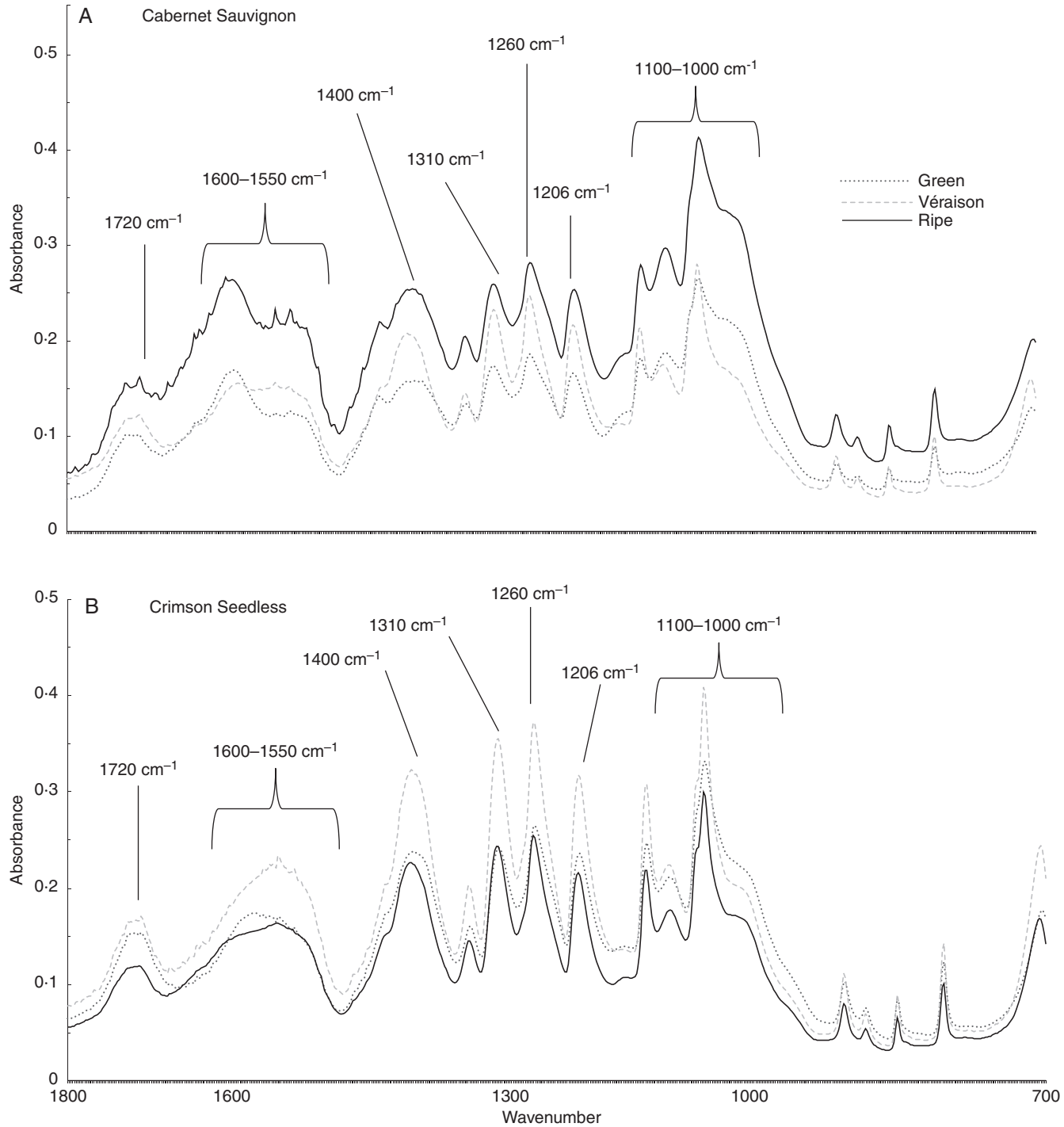

FIG. 3. Representative ATR FTIR spectral traces (from 1800 to 700 cm^{-1}) of AIR sourced from Cabernet Sauvignon (A) and Crimson Seedless (B) berries at green, véraison and ripe phases. Assignments are based on the literature, specifically Kacurakova *et al*. (2000), Stephen *et al*. (2006) and Szymanska-Chargot and Zdunek (2013). (C) Combined PCA score plot for discrimination of ripening stages in Cabernet Sauvignon and Crimson Seedless (in this case three samples per stage per cultivar are shown). Cabernet Sauvignon samples are represented as circles and Crimson Seedless samples as squares.

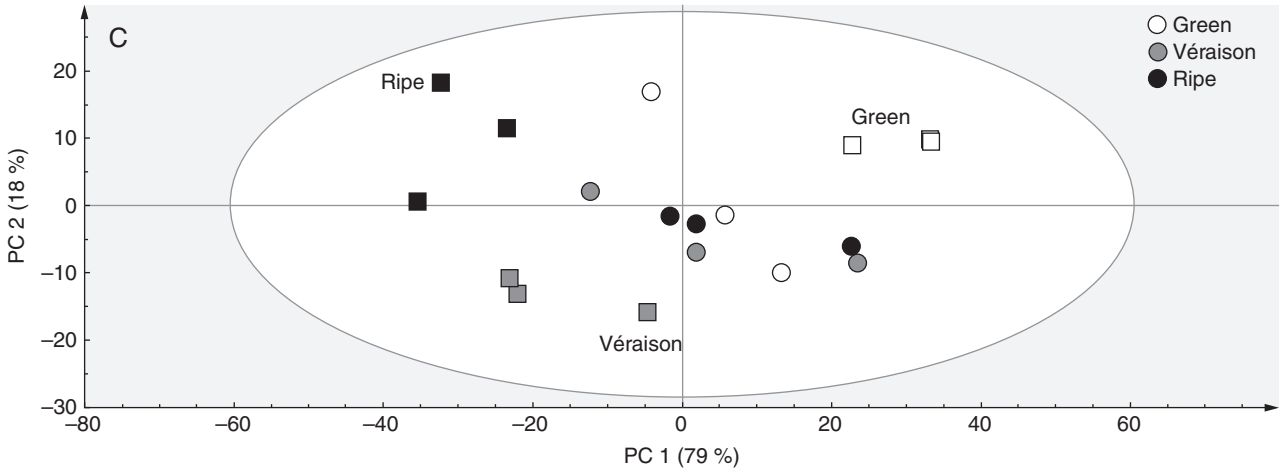

Fig. 3 *Continued*

ranged between ~10 mol % (arabinose, xylose, mannose, galactose and glucose) and ~5 mol % (rhamnose and fucose). In both wine and table grapes, galacturonic acid was found to decrease slightly, by ~5 mol %, between green and ripe stages. In contrast, galactose underwent a marked decrease with a difference of ~10–12 mol % from green to véraison to ripe walls. Slight increases, of ~5–6 mol %, were found for xylose, glucose and arabinose, whereas rhamnose, mannose and fucose did not show any change. The high galacturonic acid contents and the presence of rhamnose, arabinose and galactose suggest homogalacturonan and rhamnogalacturonan 1 (RG-I), probably mainly of pulp origin, as significant components of berry cell walls. The presence of xylose, glucose and fucose suggests xyloglucan is also present, probably from the berry skins co-extracted with the pulp tissue. Comparisons of gravimetric yields of CDTA-extractable material showed similar amounts of material extracted from Crimson Seedless and Cabernet Sauvignon at all ripening stages (Table 1). Interestingly, when comparing NaOH treatment it was found that almost twice the amount of material was extracted from Cabernet Sauvignon as from Crimson Seedless (Table 1). When comparing the monosaccharide composition analysis of both CDTA and NaOH extracts from both cultivars, very similar profiles emerged (Table 1, Fig. 2C–F). CDTA-extractable material consisted mainly of galacturonic acid (~80–90 mol %), with lower amounts of arabinose and galactose (~10–20 mol %) (Fig. 2C, D) in both cultivars. The NaOH extracts showed some differences between Cabernet Sauvignon and Crimson Seedless, particularly in mannose levels (Fig. 2E, F) but the overall composition was similar, with xylose at ~20–25 mol %, glucose at ~15–20 mol %, arabinose at ~10 mol %, galactose at ~5–10 mol % and galacturonic acid at ~10 mol % levels. Glucuronic acid was not detected in total AIR hydrosylates (Fig. 2A, B) but was detected in the CDTA and NaOH fractions (Fig. 2C–F). Developmental trends were preserved in both cultivars and no significant differences in the overall profile were evident from the analysis. However, this targeted analysis may have missed changes in bulk chemistry not measurable using degradative and chromatographic procedures; hence an alternative approach was sought.

Spectroscopic methods, using contact probes, offer a number of advantages over more precise analysis techniques. Fourier-transform infra-red (FTIR) spectroscopy is non-invasive, non-degradative and, importantly, is able to assess bulk chemistry, based on resonance overtones of chemical bonds from functional groups present in alcohol-insoluble polymers (Mouille *et al.*, 2003). Thus, in addition to carbohydrates, also detectable are proteins, phenolics and lipids if present in significant quantity. Inspection of wavelength scans from green, véraison and ripe AIR from both cultivars revealed a common sequence of bands in all fingerprints (Fig. 3A, B). Assignments of bands were based on the literature, specifically Kacurakova *et al.* (2000), Stephen *et al.* (2006) and Szymanska-Chargot and Zdunek (2013). Bands at 1720 and 1600–1550 cm^{-1} suggested the presence of carbonyls, amides and carboxyl groups associated with proteins and pectins. A number of sharp peaks were associated with pectin, including 1400 cm^{-1} for carboxyls, 1330 cm^{-1} for ring vibrations and 1260 cm^{-1} for carbonyls. Bands at 1310 cm^{-1} correspond to cellulose and those at 1206 cm^{-1} to xyloglucan and/or cellulose. All spectra also have a sharp peak with a broad shoulder around the region from 1080 to 1010 cm^{-1}, which correlates to a number of cell wall components, including pectic-β-(1,4)-galactan, arabinans, cellulose, xyloglucan and homogalacturonan, which makes interpretation incredibly difficult. The sharp peak in this region at 1064 cm^{-1} tends to correlate with xyloglucan and cellulose, while the shoulder around 1025–1017 cm^{-1} corresponds to xyloglucan and homogalacturonan resonances. Visual inspection of spectra from both cultivars and all stages show that discrimination is complicated, with differences mainly due to peak shapes and relative differences in the absorbance maxima in relation to other peaks in the same profile. Using an unsupervised approach, such as PCA, allows pattern recognition and the identification of variables (wavenumbers) that contribute to the separation achieved. FTIR spectra processed using PCA (Szymanska-Chargot and Zdunek, 2013) permitted separation of each stage (green, véraison and ripe) in a sequential fashion; however, identification of functional chemistry was less successful (Fig. 3C). It is clear, though, that FTIR coupled with PCA of grape AIR shows promise as a means to evaluate the stage of ripeness but does not provide significant insight into the subtle cell wall re-modelling events that associate with the various phases of grape ripening. A much more extensive modelling analysis is needed when reference methods are included to

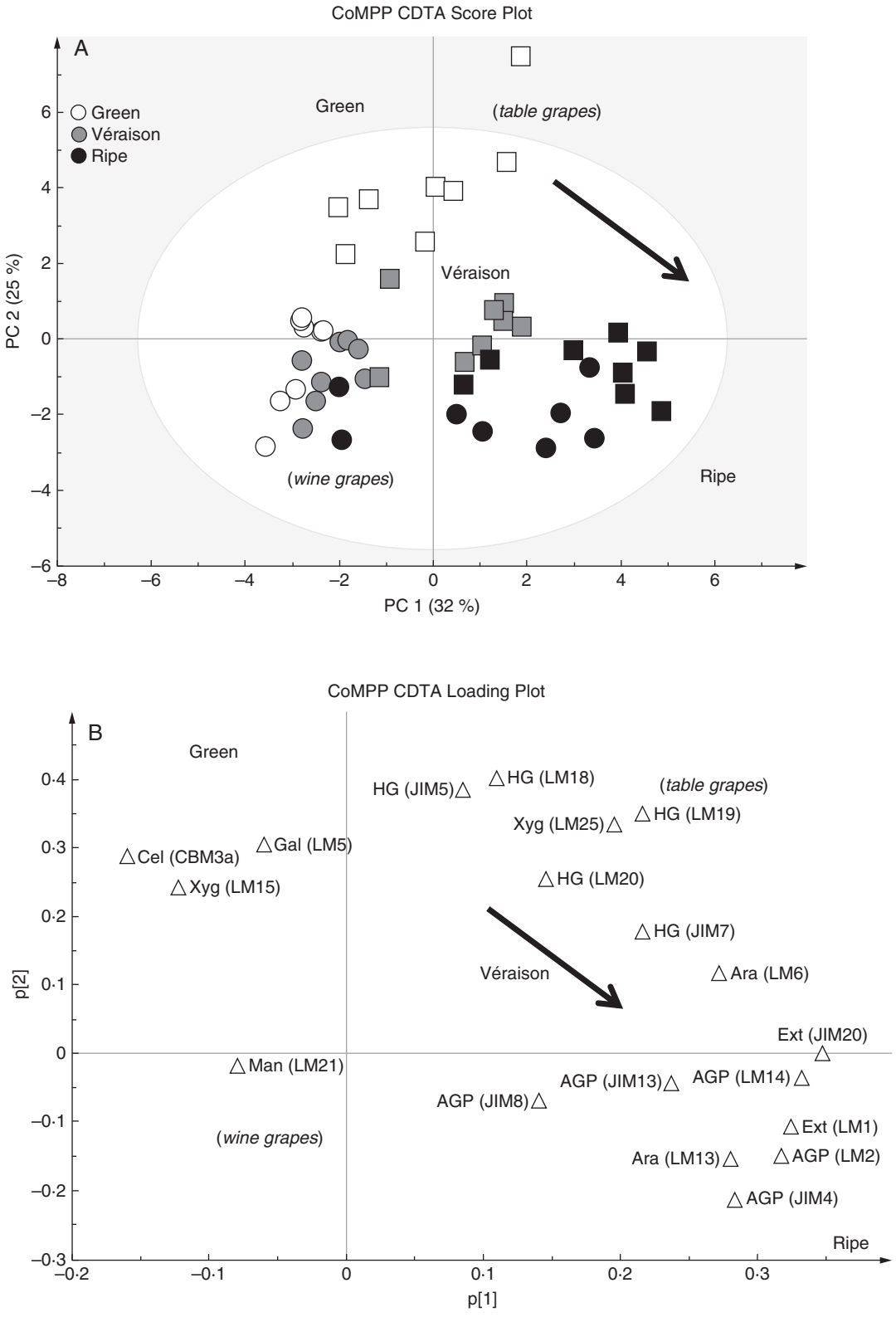

FIG. 4. CoMPP analysis of CDTA extracts prepared from green, véraison and ripe berries from Cabernet Sauvignon and Crimson Seedless vineyards. (A) PCA score plot coloured according to ripening stage (Cabernet Sauvignon samples are represented as circles and Crimson Seedless samples as squares). (B) Loading plot showing all variables (mAbs and CBMs) contributing to the separation observed. Arrows in (A) and (B) show direction of ripening. (C) Heat map showing averaged values for all probes used for CoMPP; a limit of 100 was set and a cut-off of 5 was imposed ($n = 8$ from two independent experiments).

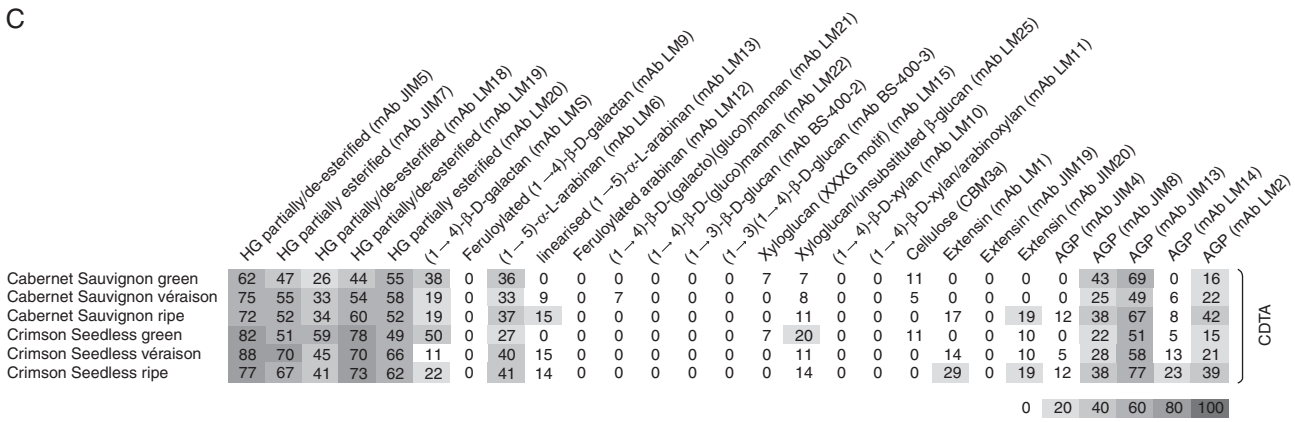

Fig. 4 *Continued*

develop partial least squares (PLS) models using a greater number of samples than currently assayed. In order to assess the subtle changes occurring in cell walls sourced from the various stages of ripening therefore requires additional, more sophisticated wall-specific techniques.

Comprehensive microarray polymer profiling is a relatively new technique in the plant cell wall field and offers the ability to provide information on polysaccharide occurrence rather than the inferred approach commonly used, based on monosaccharide ratios obtained from acidic hydrolysates of AIR. CoMPP involves the application of sets of mAbs and CBMs to detect characterized glycan epitopes known to be found on one or more cell wall polymers and/or proteins (Moller *et al*., 2007). Furthermore, because CoMPP makes use of immunological probes (detected using fluorescent labelling), the technique has higher sensitivity for subtle shifts in epitope abundance compared with the previous techniques reported on in this study. The technique involves the sequential treatment of AIR with CDTA and NaOH; the resulting solubilized material is applied to special microarray slides and probed with sets of mAbs and CBMs. The technique has been used previously to characterize tobacco (Nguema-Ona *et al*., 2012) and grapevine (Moore *et al*., 2014) leaves. Furthermore, in tobacco studies it has been shown to reveal developmental stages related to leaf age and to identify cell wall re-modelling due to grapevine polygalacturonase inhibiting protein 1 (PGIP1) expression in leaves (Nguema-Ona *et al*., 2013). Hence, the technique is well suited to the evaluation of ripening-related wall changes in various fruits, including grapes.

Firstly, CDTA extraction was performed to effectively solubilize pectin-rich material from the grape AIR. Inspection of a PCA analysis (score plot and loading plot) and the associated heat map confirmed the pectin-enriched nature of the fraction (Fig. 4A–C), as probes for homogalacturonan in various esterification states (JIM5, JIM7, LM18, LM19 and LM20), pectic-β-(1,4)-galactan (LM5), arabinans (LM6) and various AGP epitopes (JIM8, JIM13 and LM2) were found with high signal intensities (Fig. 4C). A PCA was performed on the dataset (Fig. 4A) to provide an overview of sample group separation based on ripening stage and to link this with a loading plot (Fig. 4B) to identify variables (probe IDs) that correlate with the separation. The PCA plot shows samples (both wine and table grapes) with a ripening direction from top left to(bottom right (Fig. 4A); this appeared to correspond with a gradual decrease in cellulose (CBM3a) and xyloglucan (LM15), while ripe samples showed an enrichment in wall proteins (probes for extensins and AGPs; e.g. LM1 and JIM13) (Fig. 4B, C). Interestingly, many of the homogalacturonan epitopes (e.g. JIM5, JIM7 and LM19) did not distinguish between ripening phases but rather appear to discriminate between wine and table grapes, whereas table grape samples showed a relative enrichment in these epitopes, i.e. middle to(top right of the plot (Fig. 4B). Inspection of the epitope mean values in the CDTA heat map allowed identification of ripening trends in the dataset that correlated with specific probes for homogalacturonan, RG-I and wall proteins (Fig. 4C). Probes for homogalacturonan, including JIM5, JIM7 and LM19, did not appear to change consistently between ripening stages and many increased and then decreased, remaining within ten signal values of each other; we therefore conclude that homogalacturonan levels relative to other components remain reasonably constant (Fig. 4C). Similarly, arabinans appeared to follow a constant trend (LM6) and certain AGP epitopes (JIM8 and JIM13) also decreased and then increased between stages, remaining relatively unchanged (Fig. 4C). In contrast, β-(1,4)-galactan presumably associated with pectin as in RG-I (LM5) showed a marked decrease in signal intensity from green to véraison stage and thereafter remained constant until ripe (Fig. 4C). The inverse trend was found for the extensin marker LM1, which increased at véraison and then appeared to remain constant in ripe grapes (Fig. 4c). The other interesting ripening trend was observed with the AGP probe LM2; this probe showed an increase after véraison to ripeness (Fig. 4c) and is an ideal candidate as a biomarker for ripening in grapes. We wished to further highlight (Fig. 5) the potential biomarker mAb epitopes identified in Fig. 4 by using the sizing function in the SIMCA software. Here it is possible to size each of the samples in the score plot (presented in Fig. 4A) such that each sample is assigned a symbol size proportional to its value in the non-averaged heat map dataset (not shown) (i.e. the heat map in Fig. 4C represents the average of eight biological samples). In Fig. 5 (with arrows showing the direction of ripening), three useful biomarkers in the CDTA dataset are identified: these are mAb LM5, which decreased in epitope abundance at véraison (Fig. 5A), extensin mAb LM1, which increased in epitope signal values after véraison (Fig. 5B), and mAb LM2, which

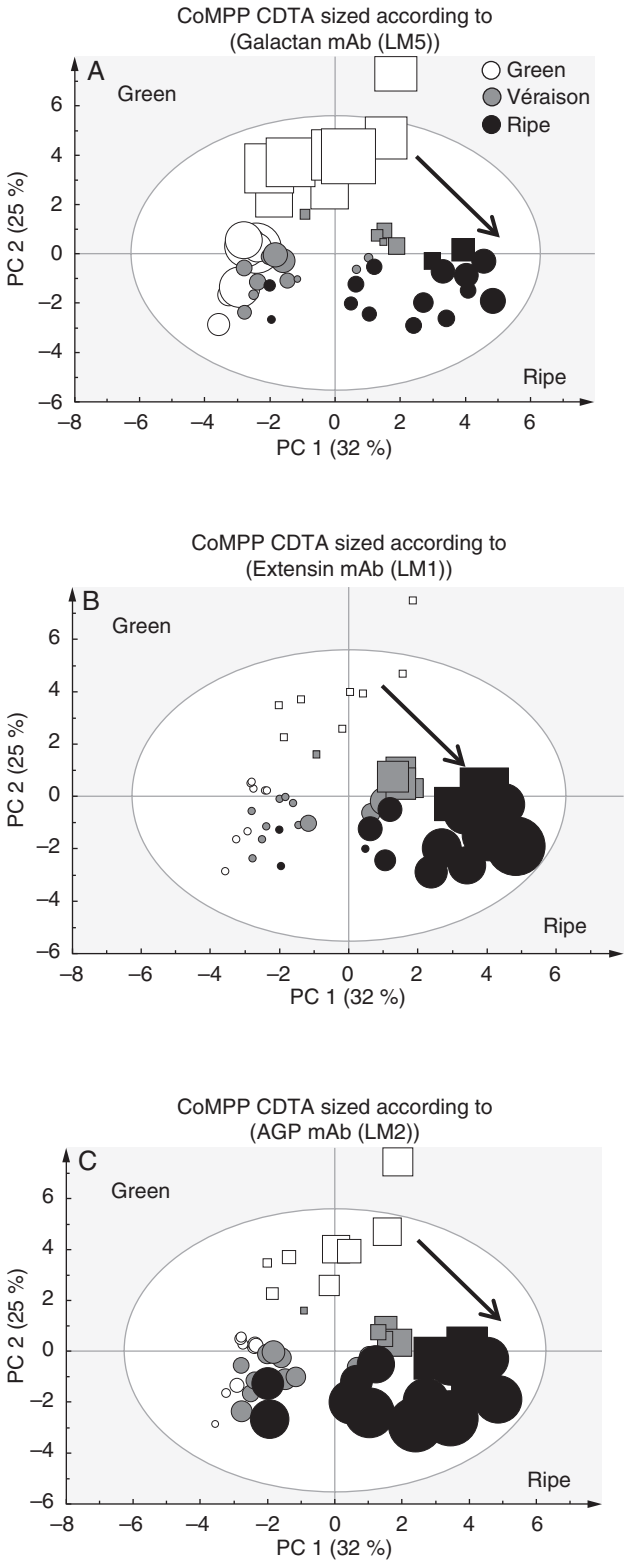

FIG. 5. Set of three PCA score plots of CoMPP data from CDTA-extracted material. See Fig. 4 for details. Cabernet Sauvignon samples are represented as circles and Crimson Seedless samples as squares. Each plot is sized according to the value of the variable: (A) mAb LM5 for pectic-β(1,4)-galactan;((B) mAb LM1 for extensin; and (C) mAb LM2 for AGP epitopes. Arrows show direction of ripening.

recognized an AGP moiety that showed the highest signal in ripe samples (Fig. 5C). However, CDTA datasets and CoMPP trends only explore half the picture; further explorations of the hemicellulose components are also necessary.

After CDTA extraction, the residual pelleted material was subjected to NaOH treatment to liberate hemicellulose polymers, which are known to bind tightly by hydrogen bonding and strong associative linkages to the cellulose microfibrils. To ascertain the broad trends (Fig. 6) present in the data, PCA was performed (as done for the CDTA values) which provides sample grouping (scores) (Fig. 6A) and impact variables (loading values) (Fig. 6B); a heat map of averaged values for all probes and samples is also provided (Fig. 6C). The NaOH application was found to extract pectic-β-(1,4)-galactan (LM5), arabinans (LM6), mannans (LM21 and LM22), xyloglucan (LM15 and LM25), cellulose (CBM3a), extensins (LM1 and JIM20) and some AGPs (JIM8, JIM13 and LM14), confirming that hemicelluloses were mainly present (Fig. 6C). Although xylans (LM10) and arabinoxylans (LM11) appeared in the extract, the values appeared highly irregular, showing no consistent trends (Fig. 6C). It is thought that these signals come from the vascular strands present in the berries forming the 'brush' (Keller, 2010); during berry picking these strands might remain in the pulp accidentally. The PCA plot of the NaOH probe values shows clear sample grouping from right to left in alignment with the direction of ripening (Fig. 6A). Comparing the score plot (Fig. 6A) with the loading plot (Fig. 6B) shows that green berries had a predominance of xyloglucan (LM15 and LM25), cellulose (CBM3a), galactans (LM5), mannans (LM21 and LM22) and tightly bound AGPs (JIM8 and JIM13), whereas ripe berries were enriched for extensins (LM1 and JIM20). Again homogalacturonan epitopes had no impact on sample grouping, whereas AGP markers (JIM8, JIM13 and LM14) appeared to account for the separation of wine grapes from table grapes (where they were proportionally more abundant) (Fig. 6A, B). The heat map values (Fig. 6C) show that pectic-β-(1,4)-galactan (LM5), mannans (LM21 and LM22), xyloglucans (LM15 and LM25) and cellulose (CBM3a) decreased significantly as ripening progressed; in comparison, the LM1 extensin epitope showed a high signal from véraison onwards (similar to that found in the CDTA fraction) while the JIM20 epitope increased slightly. The AGP epitope recognized by JIM13 showed a significant decrease from green to véraison and thereafter appeared to remain unchanged in ripe samples (Fig. 6C). The LM14 AGP epitope appeared in the NaOH dataset while generally absent in CDTA extracts, but did not appear to change during ripening (Fig. 6C). As in the pectin-enriched CDTA material, the arabinan epitope (LM6) did not show a ripening response and remained constant (Fig. 6C). As for the CDTA dataset we wished to further highlight and confirm potential biomarkers of ripening trends by using the sizing function in the SIMCA software (Fig. 7A–C). Here it is possible to size each of the samples in the score plot (presented in Fig. 6A) such that each sample is assigned a symbol size proportionate to its value in the non-averaged heatmap dataset (not shown) (i.e. the heat map in Fig. 6C represents the average of eight biological samples). Again, the mAb LM5 is highlighted, showing a strong decrease in abundance of pectic-β(1,4)-galactan epitopes from green stage to véraison (Fig. 7A). The mAb LM15, which recognizes

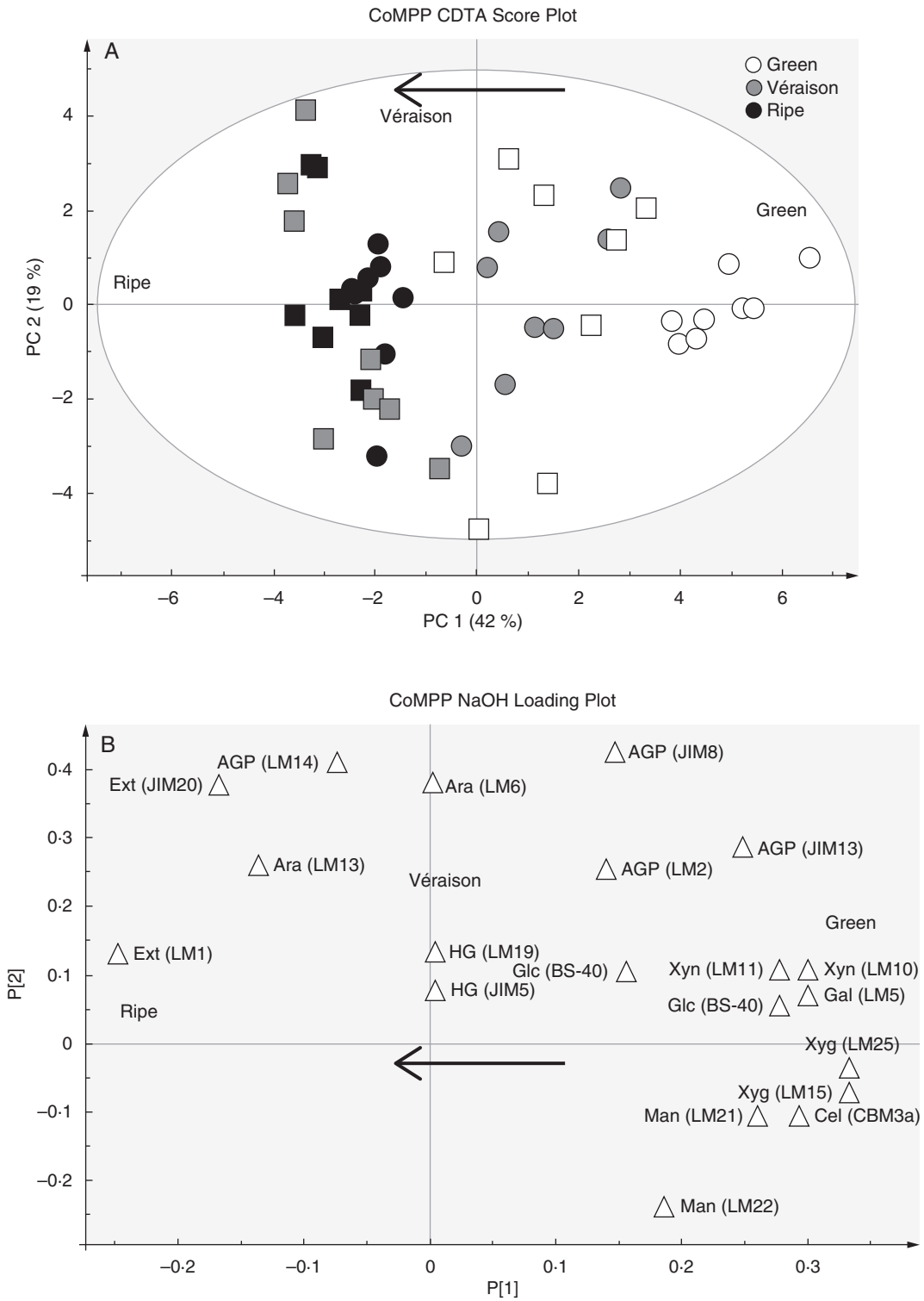

FIG. 6. CoMPP analysis of NaOH extracts prepared from green, véraison and ripe berries from Cabernet Sauvignon and Crimson Seedless vineyards. (A) PCA score plot coloured according to ripening stage. Cabernet Sauvignon samples are represented as circles and Crimson Seedless samples as squares. (B) Loading plot showing all variables (mAbs and CBMs) contributing to the separation observed. Arrows in (A) and (B) show direction of ripening. (C) Heat map showing averaged values for all probes used for CoMPP; a limit of 100 was set and a cut-off of 5 was imposed ($n = 8$ from two independent experiments).

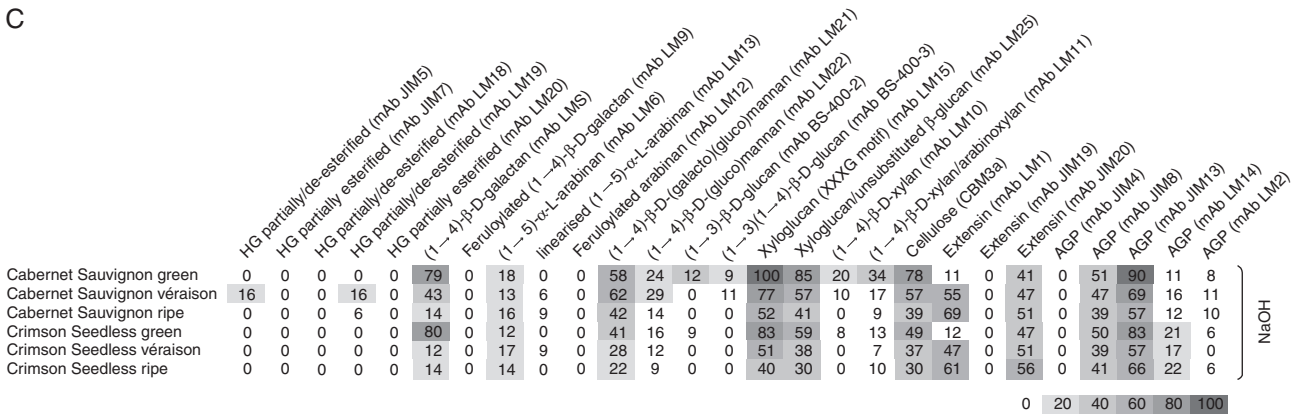

Fig. 6 *Continued*

the backbone of xyloglucan was found to show a step-wise decrease in abundance from green through véraison to ripe samples (Figs 6C and 7B). The mAb LM1 is a good candidate biomarker that recognizes an extensin moiety that accumulated at véraison and thereafter remained high in ripe berries (Figs 6C and 7C).

DISCUSSION

This study has confirmed most of the observations recorded previously regarding developmental patterns related to cell wall changes in ripening grapes. Figure 8 summarizes the key changes observed. Indeed, Saulnier and Thibault (1987*a*, *b*), Saulnier *et al.* (1988) and Vidal *et al.* (2001) showed that grapes are rich in pectin substances (composed of smooth and hairy regions) and the pulp tissue is richer in homogalacturonan, RG-I, RG-II and AGPs (Saulnier and Brioullet, 1989; Saulnier *et al.*, 1992) compared with the skins. Similarly, skin cells are rich in xyloglucans (Lecas and Brillouet, 1994) and the subunit composition has been characterized as mainly XXXG, XXFG and XLFG (Doco *et al.*, 2003*a*, *b*). Furthermore, the cell wall changes in this report correlate with those reported by Nunan *et al.* (1998), who described decreases in arabinogalactan 1 [AG1, probably pectic-β-(1,4)-galactan moieties] and xyloglucan, and slight reductions in galacturonic acid and cellulose as ripening proceeds. A similar pattern was found in a later study by Yakushiji *et al.* (2001) in which the pectin, xyloglucan and cellulose content of mesocarp tissue decreased from the green to the ripe stage.

This study has extended our knowledge of grape berry cell walls in a number of areas. Firstly, significant changes in the pectin-associated components were observed in this study, particularly the homogalacturonan and pectic-β(1,4)-galactan epitopes (Fig. 8). Interestingly, although no major differences in cell wall changes were observed between cultivars, the Crimson Seedless samples were enriched in epitopes detected by homogalacturonan-specific mAbs (Verhertbruggen *et al.*, 2009) in the CDTA fraction. Further approaches are needed, such as measuring pectin de-esterification and degradation levels between cultivars (Barnavon *et al.*, 2001), to confirm the significance of these differences. The main change appeared to be linked to pectic-β(1,4)-galactan reduction, which has been repeatedly observed in ripening fruit such as tomatoes (Lackey *et al.*, 1980) but also in many other fruits, such as blueberries (Vicente *et al.*, 2007*a*, *b*) and date palm fruit (Gribaa *et al.*, 2013). Pectic-β(1,4)-galactan reduction is also associated with growing regions such as pea stem segments (Labavitch and Ray, 1974) and azuki bean epicotyls (Nishitani and Masuda, 1979). We reported recently that tobacco leaves undergoing maturation show a staggered age-related reduction in pectic-β-(1,4)-galactan (Nguema-Ona *et al.*, 2013). The overall changes in epitope abundance of cell wall polymers in grape berries bears a strong resemblance to the composition of grape leaves (Moore *et al.*, 2014). This matches a number of studies showing pre-véraison berries performing active photosynthesis (source metabolism) until onset of ripening (véraison) and thereafter switching to become a sink (e.g. for sugars). The pectic-β(1,4)-galactan components are usually believed to associate with pectin (e.g. RG-I) but our data show mAb LM5 epitopes present in both CDTA and NaOH fractions at significant levels. Furthermore, as grape cell walls are mainly composed of pectin (homogalacturonan, RG-I and RG-II) and xyloglucan (Deng *et al.*, 2005; Yakushiji *et al.*, 2001) and it is known that pectin and xyloglucan biosynthesis co-occurs in the Golgi body (Driouich *et al.*, 2012; Atmodjo *et al.*, 2013), the relationship between these two networks in berry ripening requires further consideration.

Xyloglucan depolymerization has been observed previously (Vicente *et al.*, 2007*a*, *b*) in many fruits, including grapes (Nunan *et al.*, 1998), and we find the same pattern in our analyses (this study, Fig. 8). Significant evidence has accumulated over the past two decades concerning pectin–xyloglucan cross-links (and/or co-assembly); a useful summary of available evidence is presented in Brett *et al.* (2005). Although this is not known to occur in grapes, it is highly likely given that the occurrence of pectin–xyloglucan covalent linkages appears widespread in angiosperms (including *Arabidopsis thaliana*) (Popper and Fry, 2005). Evidence for co-assembly between pectin and xyloglucan was initially presented in maturing cauliflower stems (Waldron and Selvendran, 1992; Femenia *et al.*, 1999), but a direct covalent interaction was argued based on a number of subsequent studies (Thompson and Fry, 2000; Abdel-Missah *et al.*, 2003; Cumming *et al.*, 2005). A recent study in *Arabidopsis* has indicated that 50 % of all xyloglucan is assembled using an

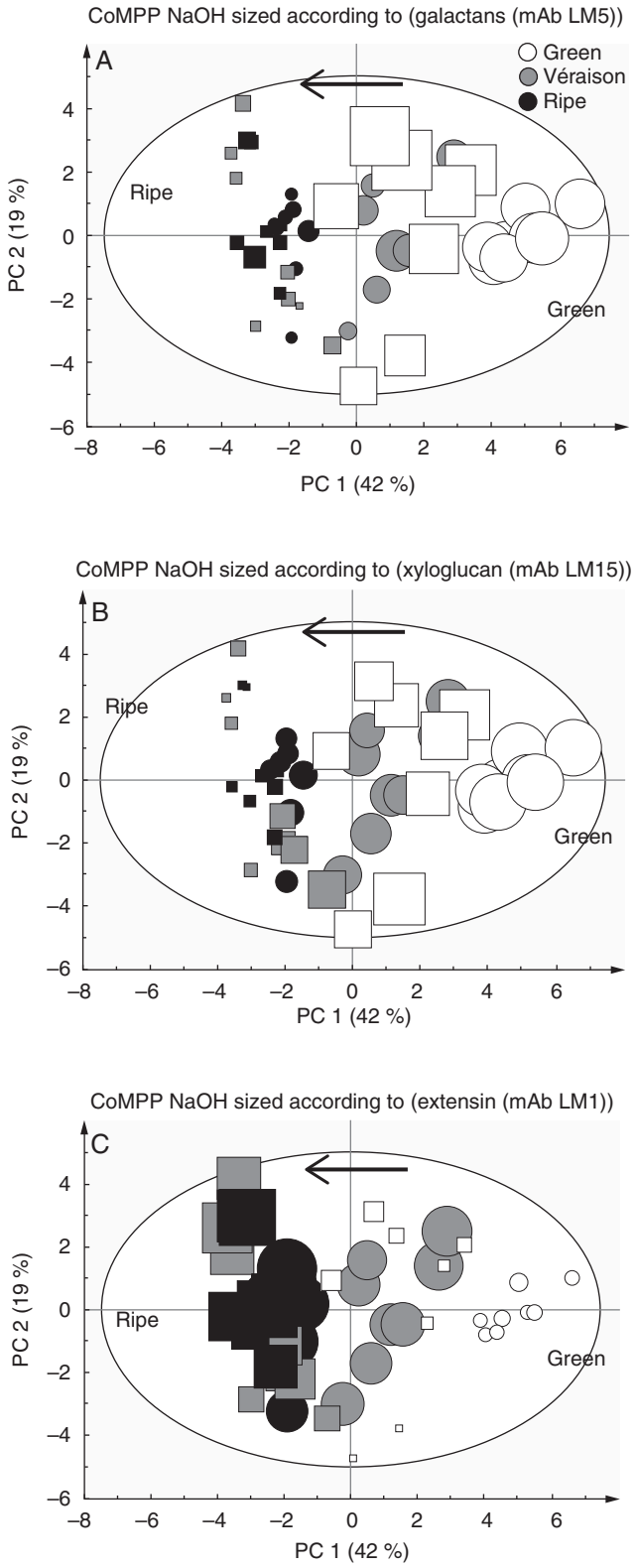

FIG. 7. A set of three PCA score plots of CoMPP data from NaOH-extracted material as detailed in Fig. 6. Cabernet Sauvignon samples are represented as circles and Crimson Seedless samples as squares. Each plot is sized according to the value of the variable: (A) mAb LM5 for pectic-β(1,4)-galactan;((B) mAb LM15 for xyloglucan; and (C) mAb LM1 for extension epitopes. Arrows show direction of ripening.

anionic primer (presumably pectin-related) and that this is necessary for positioning the oligomers in a three-dimensional network (Popper and Fry, 2008). Electrostatic bonding may be necessary to prevent neutral xyloglucan molecules from moving through the wall and dispersing into the apoplast (Abdel-Missah *et al*., 2007; Popper and Fry, 2008). Our study has also indicated that pectic-β(1,4)-galactan epitopes co-extract with the hemicellulose fraction (mainly xyloglucan) in grapes and that this is degraded/metabolized during ripening. Pectic-β(1,4)-galactan chains have not been conclusively shown to be present on xyloglucan polymers [this is suggested in Brett *et al. (*2005)], and it is known that galactose residues occur in grapevine hemicellulose (i.e. XXFG, XLFG) (Doco *et al*., 2003*a*, *b*). There is also no evidence that β-(1-2)-galactose bonds (present in galactosylated xyloglucan) are detected by mAb LM5 in addition to pectic-β(1,4)-galactan epitopes (Jones *et al*., 1997). The significance of pectic-β(1,4)-galactan present in the alkali fraction, which appears pectin-poor, is at present unclear but of considerable interest. The reduction in pectic-β(1,4)-galactan epitopes (in both CDTA and NaOH extracts) is also supported by evidence for β-galactanases (for pectin RG-I) (Buckeridge *et al*., 2005) and β-glycosidases (Buckeridge and Reid, 1994; Barnavon *et al*., 2000) being activated during seed and fruit ripening (concomitant with galactose degradation) in a number of species (Ruiz-May and Rose, 2013). β-Glycosidases have also been shown to prime xyloglucan for xyloglucan endo-transglycosylase (XET) binding/action in seeds (Buckeridge, 2010) and this correlates well with xyloglucan trans-hydrolase (XTH)/XET upregulation after véraison in grapes (when galactose levels stabilize) (Ishimaru and Kobayashi, 2002; Nunan *et al*., 2001). A recent study of tobacco seed endosperm cell walls showed that distinct layers of pectic-β(1,4)-galactan epitopes [revealed by enzyme unmasking (Marcus *et al*., 2008)] define its architectural complexity (Lee *et al*., 2013). This also highlights a shortcoming of the current study, in which we did not perform immunomicroscopy (Lee *et al*., 2011), a technique that provides an important spatial dimension to the datasets not available by using high-throughput approaches alone (Persson *et al*., 2011).

The major finding of this study concerns the changes at véraison, when extensin epitopes, specifically the mAbs LM1 (Table 1) and JIM20, significantly increased in abundance (Smallwood *et al*., 1994, 1995). This fits nicely with the observation by Nunan *et al. (*1997) that protein components rich in arginine and hydroxyproline accumulate in grapes at this stage. The JIM20 mAb (prepared from carrot cortex) is present at the same levels in all stages [in a manner analogous to *Arabidopsis thaliana* extensin 3 (AtEXT3) (Albersheim *et al*., 2011)], while the LM1 mAb shows a ripening response. The LM1 mAb was obtained from a glycoprotein of rice (*Oryza sativa*), where it is present in the cell wall and plasma membrane. This extensin deposition correlates with an oxidative burst at véraison which is believed to initiate a genetic re-programming of grapes in preparation for ripening (Pilati *et al*., 2007). Indeed, oxidative enzymes [e.g. endogenous extensin peroxidase (GvEP1)] have been shown to cross-link extensin precursors [such as monomeric extensin (Gvp1)] in grapevine callus tissue to produce an epitope recognized by JIM11 [detects carrot extensin, as shown in Smallwood *et al. (*1994)] (Jackson *et al*., 2001; Pereira *et al*., 2011). These

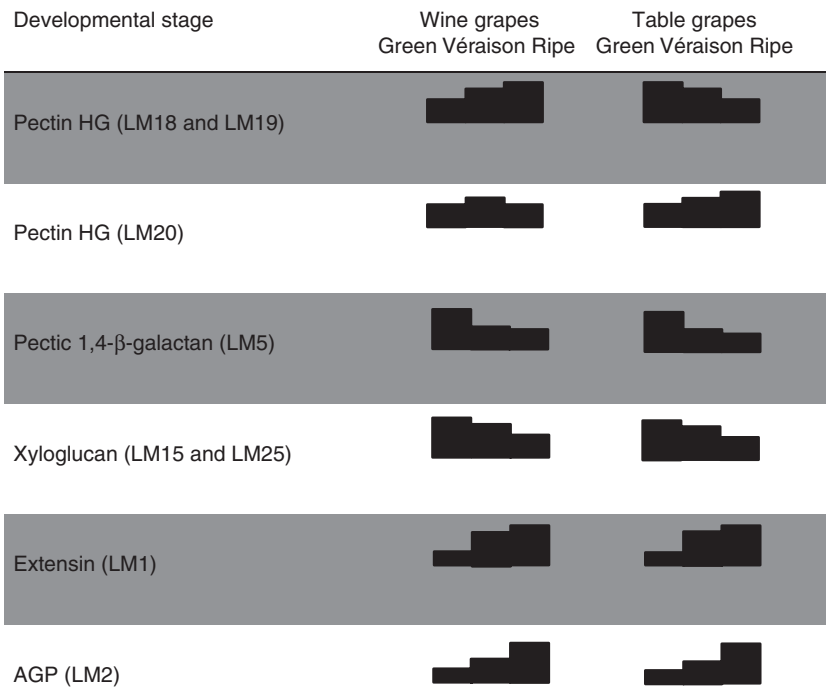

FIG. 8. Summary of selected major cell wall changes detected by specified monoclonal antibodies that occur in both wine and table grapes at green, véraison and ripe stages.

wound extensins are also known to enhance disease resistance against fungal enzymes (Ribeiro *et al*., 2006), modulate pectin properties (MacDougall *et al*., 2001) and control primary wall hydration (Pereira *et al*., 2011). Clearly, further work is necessary to confirm that such an enzyme–extensin (mAb LM1) relationship occurs in grape berries at véraison; this has only been shown in callus cultures with mAb JIM11 (Jackson *et al*., 2001; Pereira *et al*., 2011). Recently a novel protein transcription factor, VvCEB1, has been shown to control berry cell size after véraison, when rapid cell expansion occurs during sugar loading (Nicolas *et al*., 2013); it is possible, therefore, that extensins could also function to regulate the wall-related events in a related manner. Another common group of cell wall proteins are expansins; unlike extensins, these function in wall loosening rather than cross-linking, and although they are believed to be involved in grape ripening they were not evaluated in this study (Dal Santo *et al*., 2013).

AGPs constitute a major class of proteins known to accumulate in grape berries, which have received considerable attention, mostly because they accumulate in red wine during fermentation (Saulnier *et al*., 1992; Vidal *et al*., 2003; Moore and Divol, 2011); the first detailed study of AGP distribution in ripening grapes was performed by Nunan *et al.* (1998). In our data, mAbs JIM8 and JIM13 appear to show a ripening response; however, the patterns are inconsistent and probably the decreasing signal seen in ripe NaOH AIR may represent release of these glycoproteins into the apoplast. Similarly, the fact that mAbs JIM8 and JIM13 are present in high abundance in both the CDTA and the alkali fraction could mean that these AGP populations represent different locations in the cell wall, in the apoplast, and perhaps bound to and between the plasma membrane and the cell wall, and so more inaccessible, requiring covalent bond-breaking reagents for liberation (for a useful review on AGPs, see Tan *et al*., 2012). Classical AGPs are of course membrane-bound and so could require harsh reagents for liberation (Tan *et al*., 2012). Recent evidence identifying a proteoglycan in *Arabidopsis thaliana* that consists of a covalent link between an AGP, pectin and arabinoxylan (Tan *et al*., 2013) supports the idea that grape AGPs may covalently attach to other networks (e.g. xyloglucans, mannans and/or arabinoxylans), which would explain the data presented in this study. Of all the probes, the mAb LM2 shows a strong ripening response from véraison to ripe stage and detects an epitope present in rice (Smallwood *et al*., 1996); the actual moiety is an acidic trisaccharide containing glucuronic acid (Yates *et al*., 1996). The significance of this requires further investigation.

Indeed, the CoMPP analysis (Moller *et al*., 2007) performed in this study identified three excellent biomarkers for grape ripening (Fig. 8): (1) the decrease in the pectic-β(1,4)-galactan epitope from green to véraison shown by mAb LM5; (2) the increase in extensin epitopes at véraison detected by mAb LM1; and (3) the increase in AGP epitope abundance from véraison to ripe stage, seemingly specific to the mAb LM2. The combination of mAbs LM5, LM1 and LM2 appears to provide a useful means to 'type' green, véraison and ripe AIR samples; however, further confirmation of this is needed by performing a more detailed and extensive ripening study in characterized vineyards. Although we have not shown that these findings extend to other wine and table grape cultivars, these data certainly hint that this cell wall epitope distribution pattern is probably common to grapes in general. Grape ripening is a complex process involving growth not just at apical meristems, but also at lateral meristems to produce either inflorescences (flower clusters) that will develop into grape bunches or tendrils to support the liana climbing habit of the vine (Keller, 2010). How the grapevine controls the development of inflorescences and the production of berry

flesh is only just starting to be understood, with recent breakthrough molecular studies in these areas (Chaib *et al*., 2010; Fernandez *et al*., 2013), and the cell wall changes accompanying these events will undoubtedly contribute significantly to this understanding. In the context of grape ripening, the framework of the changing berry cell wall, characterized in this initial profiling study, needs to be integrated with genomic and transcriptomic studies (Goulao *et al*., 2012) (focusing on cell wall genes and enzymes) to provide a more complete model of fruit maturation in *Vitis vinifera*.

ACKNOWLEDGEMENTS

This work was supported by grants from the South African Table Grape Industry (SATI), Wine Industry Network of Expertise and Technology (Winetech), Stellenbosch University and the South African Technology and Human Resources for Industry Programme (THRIP). Pieter Raath is thanked for provision of samples and technical information on the Crimson Seedless vineyard. Chandré Joubert, Gao Yu and Jason Zhang are thanked for their technical support.

LITERATURE CITED

Abdel-Massih RM, Baydoun EAH, Brett CT. 2003. In vitro biosynthesis of 1,4-β-galactan attached to a pectin–xyloglucan complex in pea. *Planta* **216**: 502–511.

Abdel-Massih RM, Rizkallah HD, Al-Din RS, Baydoun EAH, Brett CT. 2007. Nascent pectin formed in Golgi apparatus of pea epicotyls by addition of uronic acids has different properties from nascent pectin at the stage of galactan elongation. *Journal of Plant Physiology* **164**: 1–10.

Albersheim P, Darvill A, Roberts K, Sederoff R, Staehelin A. 2011. *Plant cell walls: from chemistry to biology*. New York: Garland Science, 365–407.

Ali K, Maltese F, Fortes AM, Pais MS, Choi YH, Verpoorte R. 2011. Monitoring biochemical changes during grape berry development in Portuguese cultivars by NMR spectroscopy. *Food Chemistry* **124**: 1760–1769.

Atmodjo MA, Hao Z, Mohnen D. 2013. Evolving views of pectin biosynthesis. *Annual Review of Plant Biology* **64**: 747–779.

Baillod M, Baggiolini M. 1993. Les stades reperes de la vigne. *Revue Suisse de Viticulture, Arboriculture, Horticulture* **25**: 7–9.

Barnavon L, Doco T, Terrier N, Ageorges A, Romieu C, Pellerin P. 2000. Analysis of cell wall neutral sugar composition, β-galactosidase activity and a related cDNA clone throughout the development of *Vitis vinifera* grape berries. *Plant Physiology and Biochemistry* **38**: 289–300.

Barnavon L, Doco T, Terrier N, Ageorges A, Romieu C, Pellerin P. 2001. Involvement of pectin methyl-esterase during the ripening of grape berries: partial cDNA isolation, transcript expression and changes in the degree of methyl-esterification of cell wall pectins. *Phytochemistry* **58**: 693–701.

Brett CT, Baydoun EH, Abdel-Massih RM. 2005. Pectin–xyloglucan linkages in type I primary cell walls of plants. *Plant Biosystems* **139**: 54–59.

Buckeridge MS. 2010. Seed cell wall storage polysaccharides: models to understand cell wall biosynthesis and degradation. *Plant Physiology* **154**: 1017–1023.

Buckeridge MS, Reid JG. 1994. Purification and properties of a novel β-galactosidase or exo-(1→4)-β-D-galactanase from the cotyledons of germinated *Lupinus angustifolius* L. seeds. *Planta* 192: 502–511.

Buckeridge MS, Hutcheon IS, Reid JG. 2005. The role of exo-(1→4)-β-galactanase in the mobilization of polysaccharides from the cotyledon cell walls of *Lupinus angustifolius* following germination. *Annals of Botany* **96**: 435–444.

Chaib J, Torregosa L, Mackenzie D, Corena P, Bouquet A, Thomas MR. 2010. The grape microvine – a model system for rapid forward and reverse genetics of grapevines. *Plant Journal* **62**: 1083–1092.

Chervin C, Tira-Umphon A, Terrier N, Zouine M, Severac D, Roustan JP. 2008. Stimulation of the grape berry expansion by ethylene and effects on related gene transcripts, over the ripening phase. *Physiologia Plantarum* **134**: 534–546.

Cohen SD, Tarara JM, Gambetta GA, Matthews MA, Kennedy JA. 2012. Impact of diurnal temperature variation on grape berry development, proanthocyanidin accumulation, and the expression of flavonoid pathway genes. *Journal of Experimental Botany* **63**: 2655–2665.

Coombe BG. 1960. Relationship of growth and development to changes in sugars, auxins, and gibberellins in fruit of seeded and seedless varieties of *Vitis vinifera*. *Plant Physiology* **35**: 241–250.

Creasy GL, Creasy LL. 2009. *Grapes*. Wallingford, UK: CABI.

Cramer GR, Van Sluyter SC, Hopper DW, Pascovici D, Keighley T, Haynes PA. 2013. Proteomic analysis indicates massive changes in metabolism prior to the inhibition of growth and photosynthesis of grapevine (*Vitis vinifera* L.) in response to water deficit. *BMC Plant Biology* **13**: 49.

Cumming CM, Rizkallah HD, McKendrick KA, Abdel-Massih RM, Baydoun EA, Brett CT. 2005. Biosynthesis and cell-wall deposition of a pectin–xyloglucan complex in pea. *Planta* **222**: 546–555.

Dai ZW, Léon C, Feil R, Lunn JE, Delrot S, Gomès E. 2013. Metabolic profiling reveals coordinated switches in primary carbohydrate metabolism in grape berry (*Vitis vinifera* L.), a non-climacteric fleshy fruit. *Journal of Experimental Botany* **64**: 1345–1355.

Davies C, Robinson SP. 2000. Differential screening indicates a dramatic change in mRNA profiles during grape berry ripening. Cloning and characterization of cDNAs encoding putative cell wall and stress response proteins. *Plant Physiology* **122**: 803–812.

Davies C, Bossl PK, Gerós H, Lecourieux F, Delrot S. 2012. Source/sink relationships and molecular biology of sugar accumulation in grape berries. In: Gerós H, Chaves MM, Derot S. eds. *The biochemistry of the grape berry*. Sharjah: Bentham Science, 44–66.

Deng Y, Wu Y, Li Y. 2005. Changes in firmness, cell wall composition and cell wall hydrolases of grapes stored in high oxygen atmospheres. *Food Research International* **38**: 769–776.

Doco T, Vuchot P, Cheynier V, Moutounet M. 2003*a*. Structural modification of wine arabinogalactans during aging on lees. *American Journal of Enology and Viticulture* **54**: 150–157.

Doco T, Williams P, Pauly M, O'Neill MA, Pellerin P. 2003*b*. Polysaccharides from grape berry cell walls. Part II. Structural characterization of the xyloglucan polysaccharides. *Carbohydrate Polymers* **53**: 253–261.

Driouich A, Follet-Gueye ML, Bernard S, *et al*. 2012. Golgi-mediated synthesis and secretion of matrix polysaccharides of the primary cell wall of higher plants. *Frontiers in Plant Science* **3**: 79. , *et al*

Eyéghé-Bickong HA, Alexandersson EO, Gouws LM, Young PR, Vivier MA. 2012. Optimisation of an HPLC method for the simultaneous quantification of the major sugars and organic acids in grapevine berries. *Journal of Chromatography B, Analytical Technologies in the Biomedical and Life Sciences* **885–886**: 43–49.

Fasoli M, Dal Santo S, Zenoni S, *et al*. 2012. The grapevine expression atlas reveals a deep transcriptome shift driving the entire plant into a maturation program. *Plant Cell* **24**: 3489–3505.

Femenia A, Rigby NM, Selvendran RR, Waldron KW. 1999. Investigation of the occurrence of pectic-xylan-xyloglucan complexes in the cell walls of cauliflower stem tissues. *Carbohydrate Polymers* **39**: 151–164.

Fernandez L, Chaib J, Martinze-Zapater J-M, Thomas M, Torregrosa L. 2013. Mis-expression of a *PISTILLATA*-like MADS box gene prevents fruit development in grapevine. *Plant Journal* **73**: 918–928.

Fortes A, Agudelo-Romero P, Silva M, *et al*. 2011. Transcript and metabolite analysis in Trincadeira cultivar reveals novel information regarding the dynamics of grape ripening. *BMC Plant Biology* **11**: 149.

Goulao LF, Fernandes JC, Lopes P, Amâncio S. 2012. Tackling the cell wall of the grape berry. In Gerós H, Chaves MM, Derot S. eds. *The biochemistry of the grape berry*. Sharjah: Bentham Science, 172–193.

Gribaa A, Dardelle F, Lehner A, *et al*. 2013. Effect of water deficit on the cell wall of the date palm (*Phoenix dactylifera* 'Deglet nour', Arecales) fruit during development. *Plant, Cell and Environment* **36**: 1056–1070.

Grimplet J, Cramer GR, Dickerson JA, Mathiason K, Van Hemert J, Fennell AY. 2009. VitisNet: 'Omics' integration through grapevine molecular networks. *PLoS One* **4**: e8365.

Hervé C, Marcus SE, Knox JP. 2011. Monoclonal antibodies, carbohydrate-binding modules, and the detection of polysaccharides in plant cell walls. In: Popper Z. ed. *The plant cell wall: methods and protocols*. Berlin: Springer/Humana Press, 103–113.

Ishimaru M, Kobayashi S. 2002. Expression of a xyloglucan endotransglycosylase gene is closely related to grape berry softening. *Plant Science* **162**: 621–628.

Jackson PA, Galinha CI, Pereira CS, *et al*. 2001. Rapid deposition of extensin during the elicitation of grapevine callus cultures is specifically catalyzed by a 40-kilodalton peroxidase. *Plant Physiology* **127**: 1065–1076.

Jaillon O, Aury JM, Noel B, *et al*. 2007. The grapevine genome sequence suggests ancestral hexaploidization in major angiosperm phyla. *Nature* **449**: 463–467.

Jones L, Seymour GB, Knox JP. 1997. Localization of pectic galactan in tomato cell walls using a monoclonal antibody specific to 1,4-β-D-galactan. *Plant Physiology* **113**: 1405–1412.

Kacurakova M, Capek P, Sasinkova V, Wellner N, Ebringerova A. 2000. FT-IR study of plant cell wall model compound: pectic polysaccharides and hemicelluloses. *Carbohydrate Polymers* **43**: 195–203.

Keller M. 2010. *The science of grapevines: anatomy and physiology*. Amsterdam: Academic Press/Elsevier.

Knox JP. 1997. The use of antibodies to study the architecture and developmental regulation of plant cell walls. *International Reviews of Cytology* **171**: 79–120.

Labavitch JM, Ray PM. 1974. Turnover of cell wall polysaccharides in elongating pea stem segments. *Plant Physiology* **53**: 669–673.

Lackey GD, Gross KC, Wallner SJ. 1980. Loss of tomato cell wall galactan may involve reduced rate of synthesis. *Plant Physiology* **66**: 532–533.

Lashbrooke JG, Young PR, Dockrall SJ, Vasanth K, Vivier MA. 2013. Functional characterisation of three members of the *Vitis vinifera* L. carotenoid cleavage dioxygenase gene family. *BMC Plant Biology* **13**: 156.

Lecas M, Brillouet JM. 1994. Cell wall composition of grape berry skins. *Phytochemistry* **35**: 1241–1243.

Lee KJ, Marcus SE, Knox JP. 2011. Cell wall biology: perspectives from cell wall imaging. *Molecular Plant* **4**: 212–219.

Lee KJD, Cornuault V, Manfield IW, Ralet M-C, Knox JP. 2013. Multi-scale spatial heterogeneity of pectic rhamnogalacturonan I (RG–I) structural features in tobacco seed endosperm cell walls. *Plant Journal* **75**: 1018–1027.

Lund ST, Peng FY, Nayar T, Reid KE, Schlosser J. 2008. Gene expression analyses in individual grape (*Vitis vinifera* L.) berries during ripening initiation reveal that pigmentation intensity is a valid indicator of developmental staging within the cluster. *Plant Molecular Biology* **68**: 301–315.

MacDougall AJ, Brett GM, Morris VJ, Rigby NM, Ridout MJ, Ring SG. 2001. The effect of peptide–pectin interactions on the gelation behaviour of a plant cell wall pectin. *Carbohydrate Research* **335**: 115–126.

Marcus SE, Verhertbruggen Y, Hervé C, *et al*. 2008. Pectic homogalacturonan masks abundant sets of xyloglucan epitopes in plant cell walls. *BMC Plant Biology* **8**: 60.

Martin DM, Chiang A, Lund ST, Bohlmann J. 2012. Biosynthesis of wine aroma: transcript profiles of hydroxymethylbutenyl diphosphate reductase, geranyl diphosphate synthase, and linalool/nerolidol synthase parallel monoterpenol glycoside accumulation in Gewürztraminer grapes. *Planta* **236**: 919–929.

Martínez-Esteso MJ, Vilella-Antón MT, Pedreño MÁ, Valero ML, Bru-Martínez R. 2013. iTRAQ-based protein profiling provides insights into the central metabolism changes driving grape berry development and ripening. *BMC Plant Biology* **13**: 167.

Moller I, Sørensen I, Bernal AJ, *et al*. 2007. High-throughput mapping of cell-wall polymers within and between plants using novel microarrays. *Plant Journal* **50**: 1118–1128.

Moore JP, Divol B. 2011. Tracking the careers of grape and wine polymers using biotechnology and systems biology. In: Bagchi D, Lau FC, Ghosh DK. eds. *Biotechnology in functional foods and nutraceuticals*. Boca Raton: CRC Press, 389–406.

Moore JP, Nguema-Ona E, Fangel JU, Willats WG, Hugo A, Vivier MA. 2014. Profiling the main cell wall polysaccharides of grapevine leaves using high-throughput and fractionation methods. *Carbohydrate Polymers* **99**: 190–198.

Mouille G, Robin S, Leconte M, Pagant S, Höfte H. 2003. Classification and identification of *Arabidopsis* cell wall mutants using Fourier-transform infrared (FT-IR) micro-spectroscopy. *Plant Journal* **35**: 393–404.

Nguema-Ona E, Moore JP, Fagerström A, *et al*. 2012. Profiling the main cell wall polysaccharides of tobacco leaves using high-throughput and fractionation techniques. *Carbohydrate Polymers* **88**: 939–949.

Nguema-Ona E, Moore JP, Fagerström AD, *et al*. 2013. Overexpression of the grapevine PGIP1 in tobacco results in compositional changes in the leaf arabinoxyloglucan network in the absence of fungal infection. *BMC Plant Biology* **13**: 1–15.

Nicolas P, Lecourieux D, Gomès E, Delrot S, Lecourieux F. 2013. The grape berry-specific basic helix–loop–helix transcription factor VvCEB1 affects cell size. *Journal of Experimental Botany* **64**: 991–1003.

Nishitani K, Masuda Y. 1979. Growth and cell wall changes in azuki bean epicotyls I. Changes in wall polysaccharides during intact growth. *Plant and Cell Physiology* **20**: 63–74.

Nunan KJ, Sims IM, Bacic A, Robinson SP, Fincher GB. 1997. Isolation and characterization of cell walls from the mesocarp of mature grape berries (*Vitis vinifera*). *Planta* **203**: 93–100.

Nunan KJ, Sims IM, Bacic A, Robinson SP, Fincher GB. 1998. Changes in cell wall composition during ripening of grape berries. *Plant Physiology* **118**: 783–792.

Nunan KJ, Davies C, Robinson SP, Fincher GB. 2001. Expression patterns of cell wall-modifying enzymes during grape berry development. *Planta* **214**: 257–264.

Peppi CM, Fidelibus MW, Dokoozlian N. 2006. Abscisic acid application and concentration affect firmness, pigmentation, color of 'Flame Seedless' grapes. *HortScience* **41**: 1440–1445.

Pereira C, Ribeiro J, Vatulescu A, Findlay K, MacDougall A, Jackson P. 2011. Extensin network formation in *Vitis vinifera* callus cells is an essential and causal event in rapid and H_2O_2-induced reduction in primary cell wall hydration. *BMC Plant Biology* **11**: 106.

Persson S, Sorensen I, Moller I, Willats W, Pauly M. 2011. Dissection of plant cell walls by high-throughput methods. *Annual Plant Reviews: Plant Polysaccharides: Biosynthesis and Bioengineering* **41**: 43–64.

Pilati S, Perazzolli M, Malossini A, Cestaro A, *et al*. 2007. Genome-wide transcriptional analysis of grapevine berry ripening reveals a set of genes similarly modulated during three seasons and the occurrence of an oxidative burst at véraison. *BMC Genomics* **8**: 428.

Popper ZA, Fry SC. 2005. Widespread occurrence of a covalent linkage between xyloglucan and acidic polysaccharides in suspension-cultured angiosperm cells. *Annals of Botany* **96**: 91–99.

Popper ZA, Fry SC. 2008. Xyloglucan-pectin linkages are formed intraprotoplasmically, contribute to wall-assembly, and remain stable in the cell wall. *Planta* **227**: 781–794.

Ribeiro JM, Pereira CS, Soares NC, Vieira AM, Feijó JA, Jackson PA. 2006. The contribution of extensin network formation to rapid, hydrogen peroxide-mediated increases in grapevine callus wall resistance to fungal lytic enzymes. *Journal of Experimental Botany* **57**: 2025–2035.

Rolle L, Siret R, Segade SR, Maury C, Gerbi V, Jourjon F. 2012. Instrumental texture analysis parameters as markers of table-grape and wine-grape quality: a review. *American Journal of Enology and Viticulture* **63**: 1–27.

Ruiz-May E, Rose JK. 2013. Cell wall architecture and metabolism in ripening fruit and the complex relationship with softening. In: Seymour G, Tucker GA, Poole M, Giovannoni J. eds. *The molecular biology and biochemistry of fruit ripening*. Wiley-Blackwell, 163–187.

Dal Santo S, Vannozzi A, Tornielli GB, *et al*. 2013. Genome-wide analysis of the expansin gene superfamily reveals grapevine-specific structural and functional characteristics. *PLoS One* **8**: e62206.

Santo SD, Tornielli GB, Zenoni S, *et al*. 2013. The plasticity of the grapevine berry transcriptome. *Genome Biology* **14**: r54.

Saulnier L, Brillouet JM. 1989. An arabinogalactan-protein from the pulp of grape berries. *Carbohydrate Research* **188**: 137–144.

Saulnier L, Thibault JF. 1987*a*. Enzymic degradation of isolated pectic substances and cell wall from pulp of grape berries. *Carbohydrate polymers* **7**: 345–360.

Saulnier L, Thibault JF. 1987*b*. Extraction and characterization of pectic substances from pulp of grape berries. *Carbohydrate Polymers* **7**: 329–343.

Saulnier L, Brillouet JM, Joseleau JP. 1988. Structural studies of pectic substances from the pulp of grape berries. *Carbohydrate Research* **182**: 63–78.

Saulnier L, Brillouet JM, Moutounet M, du Penhoat CH, Michon V. 1992. New investigations of the structure of grape arabino-galactan-protein. *Carbohydrate Research* **224**: 219–235.

Seymour GB, Østergaard L, Chapman NH, Knapp S, Martin C. 2013*a*. Fruit development and ripening. *Annual Review of Plant Biology* **64**: 219–241.

Seymour GB, Chapman NH, Chew BL, Rose JKC. 2013*b*. Regulation of ripening and opportunities for control in tomato and other fruits. *Plant Biotechnology Journal* **11**: 269–278.

Singleton VL, Trousdale EK. 1992. Anthocyanin-tannin interactions explaining differences in polymeric phenols between white and red wines. *American Journal of Enology and Viticulture* **43**: 63–70.

Smallwood M, Beven A, Donovan N, *et al*. 1994. Localization of cell wall proteins in relation to the developmental anatomy of the carrot root apex. *Plant Journal* **5**: 237–246.

Smallwood M, Martin H, Knox JP. 1995. An epitope of rice threonine- and hydroxyproline-rich glycoprotein is common to cell wall and hydrophobic plasma-membrane glycoproteins. *Planta* **196**: 510–522.

Smallwood M, Yates EA, Willats WG, Martin H, Knox JP. 1996. Immunochemical comparison of membrane-associated and secreted arabinogalactan-proteins in rice and carrot. *Planta* **198**: 452–459.

Stephen AM, Phillips GO, Williams P. 2006. *Food polysaccharides and their applications.* Boca Raton: CRC Press.

Szymanska-Chargot M, Zdunek A. 2013. Use of FT-IR spectra and PCA for the bulk characterization of cell wall residues of fruits and vegetables along a fraction process. *Food Biophysics* **8**: 1–14.

Tan L, Showalter AM, Egelund J, Hernandez-Sanchez A, Doblin MS, Bacic A. 2012. Arabinogalactan-proteins and the research challenges for these enigmatic plant cell surface proteoglycans. *Frontiers in Plant Science* **3**: 140.

Tan L, Eberhard S, Pattathil S, *et al*. 2013. An *Arabidopsis* cell wall proteoglycan consists of pectin and arabinoxylan covalently linked to an arabinogalactan protein. *Plant Cell* **25**: 270–287.

Terrier N, Glissant D, Grimplet J, *et al*. 2005. Isogene specific oligo-arrays reveal multifaceted changes in gene expression during grape berry (*Vitis vinifera* L.) development. *Planta* **222**: 832–847.

Thomas TR, Shackel KA, Matthews MA. 2008. Mesocarp cell turgor in *Vitis vinifera* L. berries throughout development and its relation to firmness, growth, and the onset of ripening. *Planta* **228**: 1067–1076.

Thompson JE, Fry SC. 2000. Evidence for covalent linkage between xyloglucan and acidic pectins in suspension-cultured rose cells. *Planta* **211**: 275–286.

Verhertbruggen Y, Marcus SE, Haeger A, Ordaz-Ortiz JJ, Knox JP. 2009. An extended set of monoclonal antibodies to pectic homogalacturonan. *Carbohydrate Research* **344**: 1858–1862.

Vicente AR, Saladie M, Rose JKC, Labavitch JM. 2007*a*. The linkage between cell wall metabolism and fruit softening. *Journal of the Science of Food and Agriculture* **87**: 1435–1448.

Vicente AR, Ortugno C, Rosli H, Powell AL, Greve L, Labavitch JM. 2007*b*. Temporal sequence of cell wall disassembly events in developing fruits. 2. Analysis of blue berry (*Vaccinium* species). *Journal of Agricultural and Food Chemistry* **55**: 4125–4130.

Vidal S, Williams P, O'Neill MA, Pellerin P. 2001. Polysaccharides from grape berry cell walls. Part I: tissue distribution and structural characterization of the pectic polysaccharides. *Carbohydrate Polymers* **45**: 315–323.

Vidal S, Williams P, Doco T, Moutounet M, Pellerin P. 2003. The polysaccharides of red wine: total fractionation and characterization. *Carbohydrate Polymers* **54**: 439–447.

Waldron KW, Selvendran RR. 1992. Cell wall changes in immature asparagus stem tissue after excision. *Phytochemistry* **31**: 1931–1940.

Yakushiji H, Sakurai N, Morinaga K. 2001. Changes in cell-wall polysaccharides from the mesocarp of grape berries during véraison. *Physiologia Plantarum* **111**: 188–195.

Yates E, Valdor JF, Haslam SM, *et al*. 1996. Characterisation of carbohydrate structural features recognized by anti-arabinogalactan-protein monoclonal antibodies. *Glycobiology* **6**: 131–139.

York WS, Darvill AG, McNeil M, Stevenson TT, Albersheim P. 1985. Isolation and characterization of plant cell walls and cell wall components. *Methods in Enzymology* **118**: 3–40.

Young P, Lashbrooke J, Alexandersson E, *et al*. 2012. The genes and enzymes of the carotenoid metabolic pathway in *Vitis vinifera* L. *BMC Genomics* **13**: 243.

Zouine M, Latché A, Rousseau C, *et al*. 2012. The tomato genome sequence provides insights into fleshy fruit evolution. *Nature* **485**: 635–641.

Zouid I, Siret R, Jourjon F, Mehinagic E, Rolle L. 2013. Impact of grapes heterogeneity according to sugar level on both physical and mechanical berries properties and their anthocyanin extractability at harvest. *Journal of Texture Studies* **44**: 95–103.